Biological Probes

Deutsche Ausgabe: DOI: 10.1002/ange.201500008
Internationale Ausgabe: DOI: 10.1002/anie.201500008

Construction of an Upconversion Nanoprobe with Few-Atom Silver Nanoclusters as the Energy Acceptor**

*Yan Xiao, Lingyu Zeng, Tian Xia, Zhengjun Wu, and Zhihong Liu**

Abstract: *Herein we report that few-atom silver nanoclusters (Ag NCs) can be effective energy acceptors for upconversion phosphors (UCPs). A luminescence resonance energy transfer (LRET) probe for biothiols was constructed by decorating UCPs with dithiol-stabilized Ag NCs. Owing to the unique properties of ultrasmall NCs, properties which bridge the gap between those of small molecules and those of nanoparticles, the use of approximately 1.9 nm Ag NCs as energy acceptors endows the probe with high energy-transfer efficiency, good biocompatibility, and flexibility. The UCP–Ag NC nanoprobe enables rapid and robust target assay in solutions. It was also uploaded into living cells and used to detect intracellular biothiol levels with high discrimination. Moreover, the probe shows transportability in vivo and can be used for tissue imaging. The facile growth of few-atom metal NCs on diverse templates may enable the development of various nanoprobes combining UCPs and metal NCs.*

Upconversion phosphors (UCPs) are promising luminescent materials for the construction of nanoprobes for application in living systems owing to their features of excitation with near-infrared (NIR) light and anti-Stokes emission.[1] Generally, UCPs are decorated with an energy acceptor to form the probe, in which the emission of UCPs is tuned by luminescence resonance energy transfer from the UCP (the energy donor) to the energy acceptor.[2] In some other types of hybrid systems, UCPs are combined with optical materials to enhance the luminescence of UCPs.[3] The properties of the energy acceptor or optical material usually play the key role in the performance of nanoprobes. To date, a variety of upconversion LRET systems based on organic dyes[4] and inorganic materials, including carbon nanomaterials,[5] metal nanoparticles,[6] and 2D covalent-network solids,[7] as energy acceptors have been developed with considerable success. Nevertheless, organic molecules as energy acceptors always fall short on energy-transfer efficiency, whereas inorganic energy acceptors tend to be less flexible and less biocompatible. Hence, there is still great demand for new energy acceptors for UCPs that meet comprehensive goals for probe performance.

Recently, few-atom noble-metal nanoclusters (NCs) have attracted increasing attention for their unique material properties that bridge the gap between those of small molecules and those of nanoparticles.[8] The high sensitivity of metal NCs to their environment offers the opportunity for application in biological and chemical probes.[9] Furthermore, metal NCs can be grown on various templates, such as proteins, DNA, and polymers, which enables facile assembly with other materials through either covalent or noncovalent bonds. Most recently, we discovered that the ultrasmall silver nanoclusters exhibit pronounced energy-accepting capability to quench a luminophore.[10] These findings suggest the possibility of using ultrasmall metal NCs as the energy acceptor of an upconversion nanoprobe, with which both the favorable biocompatibility and flexibility of small-molecule energy acceptors and the high energy-transfer efficiency featured by nanomaterial acceptors should be possible.

We herein report an NIR nanoprobe containing ultrasmall Ag NCs stabilized with a dithiol ligand as the energy acceptors of UCPs. The UCP–Ag NC nanoprobe was designed with a core–satellite structure, in which each UCP nanosphere core is surrounded by a few Ag NCs (Figure 1). The two parts were assembled by an electrostatic interaction, a simple yet reliable connection with successful applications in cells and the body,[1d,11] between positively charged polyethylenimine (PEI)-coated UCPs ($NaYF_4$:Yb,Tm) and neg-

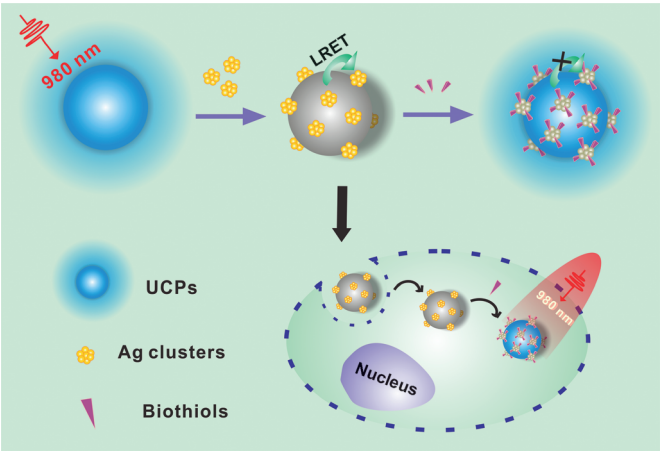

Figure 1. Structure and sensing mechanism of the upconversion nanoprobe with silver nanoclusters as energy acceptors for the detection of biothiols.

[*] Y. Xiao, L. Zeng, Z. Wu, Dr. Z. Liu
Key Laboratory of Analytical Chemistry for Biology and Medicine (Ministry of Education)
College of Chemistry and Molecular Sciences
Wuhan University, Wuhan 430072 (P. R. China)
E-mail: zhhliu@whu.edu.cn
T. Xia
College of Life Science, Wuhan University
Wuhan 430072 (P. R. China)

[**] This research was supported by the National Natural Science Foundation of China (No. 21375098). We are grateful to Prof. Xueyuan Chen and Dr. Datao Tu for their help with lifetime measurements.

Supporting information for this article is available on the WWW under http://dx.doi.org/10.1002/anie.201500008.

atively charged Ag NCs stabilized by *meso*-2,3-dimercaptosuccinic acid (DMSA). The DMSA-stabilized Ag NCs show an intense absorption peak around 500 nm that matches well with the emission of $NaYF_4$:Yb,Tm phosphors at 450–500 nm as a result of $^1D_2 \rightarrow {}^3F_4$ and $^1G_4 \rightarrow {}^3H_6$ transitions of Tm[12] (see Figure S1 in the Supporting Information), thereby enabling LRET from UCPs to Ag NCs and thus quenching of the luminescence of the UCPs. As a proof-of-concept application, we chose biothiols as the targets and thus made direct use of the specific chemistry of thiols and silver.[13] The total concentration of thiols is essential for maintaining the appropriate redox status of cells.[14] Therefore, the detection of the amount of biothiols in cells and tissues is significant. The reaction of Ag NCs with thiols should alter the light absorption of Ag NCs and lead to inhibition of the energy transfer from UCPs to Ag NCs. As a consequence, the upconversion luminescence (UCL) of UCPs should differ according to the amount of thiols present. The design could therefore lead to a simple and rapid mix-and-read assay protocol for thiols. More importantly, the ultrasmall Ag NCs possess excellent water solubility and higher thermodynamic stability and biocompatibility than previously reported large-scale nanosized energy acceptors. These features are favorable for applications in cells and the body.

We synthesized oleic acid coated UCPs (OA-UCPs) by a solvothermal method[7] and characterized the product by transmission electron microscopy (TEM), X-ray powder diffraction (XRD), and Fourier transform infrared (FTIR) spectroscopy. TEM revealed that the as-prepared OA-UCPs had a fairly uniform size and an average diameter of about 30 nm (see Figure S2 a). The XRD pattern indicated that the peak positions and intensities of the nanocrystals agreed well with the calculated values of pure hexagonal-phase $NaYF_4$ nanocrystals (see Figure S2 b). The crystalline phase was also confirmed by a high-resolution (HR) TEM image, which showed a typical *d*-spacing value of 0.52 nm, corresponding to the (100) plane of a β-phase $NaYF_4$ layer (see Figure S2 c). The presence of OA molecules on the surface of the UCPs was verified by FTIR spectroscopy (see Figure S2 d). To make the UCPs hydrophilic for further biological applications, we modified the originally synthesized hydrophobic UCPs with PEI by a ligand-exchange procedure.[15] This modification strategy coats the particles with amino groups and thus not only ensures good water solubility but also makes the UCPs positively charged under neutral pH conditions so as to facilitate the assembly with negatively charged Ag NCs. Functionalization with PEI was also verified by FTIR spectroscopy (see Figure S2 d). Furthermore, TEM images indicated no significant changes in size, shape, and crystallinity of the UCPs after modification with PEI (see Figure S3).

The DMSA-protected ultrasmall Ag NCs were prepared according to a method reported previously,[16] and the product was characterized in detail by TEM, XRD, and various spectroscopic methods. The UV/Vis spectrum of the as-prepared Ag NCs exhibited a sharp absorption peak at 500 nm and a shoulder around 620 nm (see Figure S1), in agreement with previously reported results, thus indicating the generation of ultrasmall metal nanoclusters.[16] The molar absorption coefficient of the Ag NCs at 500 nm, as calculated on the basis of the concentration-dependent absorbance, was $1 \times 10^4\ L\,mol^{-1}\,cm^{-1}$ (see Figure S4). The X-ray diffraction pattern confirmed the formation of small clusters with high purity, since it showed no characteristic peaks of large-size silver nanoparticles or bulk silver (see Figure S5 a). The average size of the prepared Ag NCs was approximately 1.9 nm, as revealed by TEM (see Figure S5 b). The X-ray photoelectron spectroscopy (XPS) survey spectrum of the clusters showed the presence of the expected elements, C, S, O, and Ag (see Figure S6 a). The Ag 3d peak between Ag^+ (367.5 eV) and Ag^0 (368.2 eV) and the S 2p peak at 162.0 eV confirmed the formation of silver atomic clusters protected by thiol ligands (see Figure S6 b,c). The protection of the clusters by DMSA ligands was further verified by FTIR spectroscopic analysis. The absorption of the ligand itself at the S–H stretching frequency of $2550\ cm^{-1}$ disappeared in the spectrum of DMSA-Ag NCs, thus indicating the binding of Ag atoms by the ligand through the formation of S–Ag bonds (see Figure S7).

To evaluate the feasibility of utilizing Ag NCs as the energy acceptor of UCPs, we first examined the quenching of UCP emission by Ag NCs. After loading of the PEI-modified UCPs with Ag NCs through electrostatic interactions, the upconversion luminescence of UCPs was quenched gradually according to the increase in the concentration of Ag NCs, thus indicating the occurrence of energy transfer from UCPs to Ag NCs (Figure 2 a). Notably, in the presence of a small amount ($25\ \mu g\,mL^{-1}$) of Ag NCs, the emission of the UCPs was quenched to a degree close to 80 % (Figure 2 b), which is difficult to achieve with small-molecule energy acceptors and indicates a pronounced luminescence-quenching ability of Ag NCs that is comparable to that of most inorganic nanosized energy acceptors. To confirm the resonance energy transfer from UCPs to Ag NCs, we performed luminescence-lifetime measurements. The lifetime of the 480 nm emission of UCPs was reduced from 686 to 467 μs upon the introduction of Ag NCs (see Figure S8 a), thus indicating the occurrence of resonance energy transfer. Furthermore, the quenching kinetics of the system suggests that the assembly of the UCPs with Ag NCs is a quite fast process that reaches equilibrium in about 10 min (see Figure S8 b). The absorption wavelength of Ag NCs, as reported previously, can be adjusted by using different templates, thus ensuring adaptability to other kinds of UCPs. To provide more direct evidence of the decoration of the surface of UCPs with Ag NCs, we further conducted TEM and ζ-potential analysis. A core–satellite structure of the probe could be clearly seen in the TEM and HRTEM images (see Figure S8 c,d). The ζ potentials of as-prepared PEI-coated UCPs and DMSA-protected Ag NCs were +50.1 and −36.4 mV, respectively. After assembly, the ζ potential of the nanoprobe was observed at −6.55 mV, thus confirming the occurrence of charge neutralization between the two oppositely charged components (see Figure S9). Considering the possible uptake of the probe by endocytosis in cell experiments, we also checked the ζ potential and the size distribution of the nanoprobe at acidic pH values (6.5–4.5). The results showed that the particles tend to aggregate slightly as the pH value

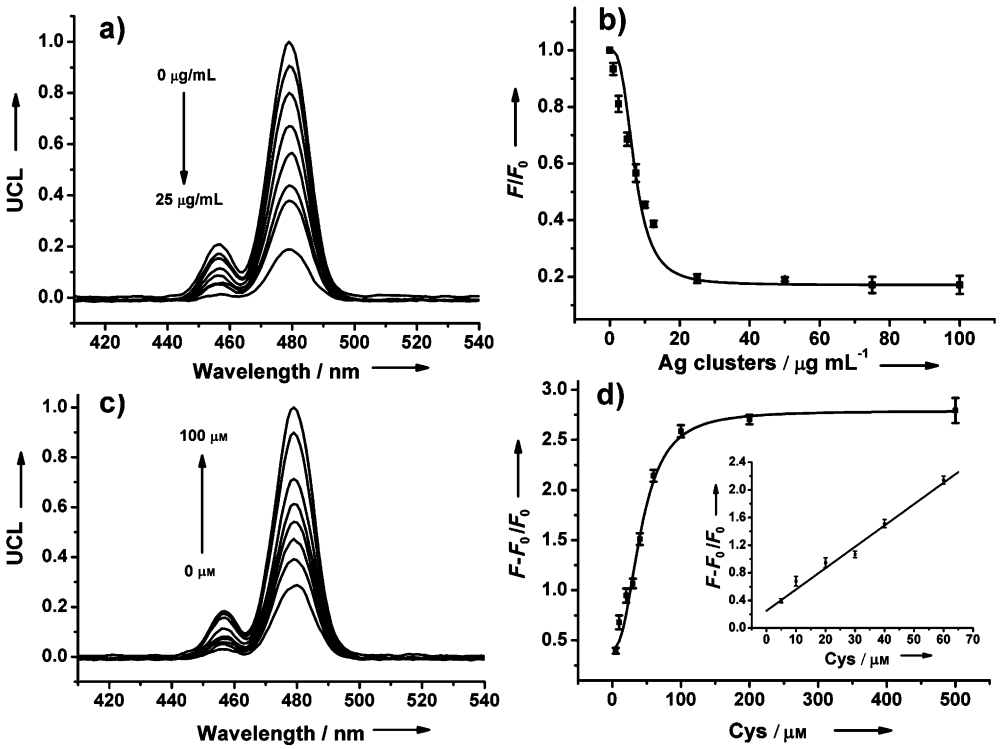

Figure 2. a) Emission of PEI-UCPs (30 μg mL^{-1}) in the presence of different concentrations of DMSA-Ag NCs. b) Relative fluorescence intensity (F/F_0, in which F and F_0 are the emission intensity of PEI-UCPs in the presence and absence of DMSA-Ag NCs, respectively) of PEI-UCPs in the presence of varying amounts of DMSA-Ag NCs (0, 1, 2.5, 5, 7.5, 10, 12.5, 25, 50, 75, and 100 μg mL^{-1}). c) Emission of the nanoprobe in the presence of different concentrations of Cys. d) Relative fluorescence intensity ($(F-F_0)/F_0$) of the nanoprobe in response to varying concentrations of Cys (5, 10, 20, 30, 40, 60, 100, 200, and 500 μM).

decreases (see Table S1 in the Supporting Information), which is consistent with a previous report.[17]

We next performed a biothiols assay with the UCP–Ag NC probe and cysteine (Cys) as a model target in an aqueous solution. With the addition of an increasing amount of Cys to the probe solution, the emission intensity of the UCPs at 480 nm was recovered gradually (Figure 2c) as a result of inhibition of the energy transfer from UCPs to Ag NCs. The relative fluorescence intensity of the nanoprobe ($(F-F_0)/F_0$, in which F and F_0 are the emission intensity of the nanoprobe in the presence and absence of target molecules, respectively) is dependent on the concentration of Cys (Figure 2d). The change in energy-transfer efficiency can be explained by the altered light absorption of the Ag NCs. Upon the reaction with biothiols, the absorption peak of the Ag NCs at 500 nm decreased drastically in intensity, and there was a clear change in the solution color (see Figure S10). The decrease in absorption of the Ag NCs impairs the spectral match between the donor–acceptor pair and is responsible for the inhibition of the LRET process. This upconversion nanoprobe based on Ag NCs exhibits the remarkable advantage that the assay is highly robust with satisfying reproducibility and stability, as shown by the low deviations in Figure 2d. The robustness of the assay can be attributed to the merits of the ultrasmall NCs: 1) The good water solubility of Ag NCs leads to thermodynamic stability of the assay system; 2) the nonspecific adsorption of sensing targets on the probe is minimized because of the ultrasmall size of Ag NCs. These merits thus allow for a rapid mix-and-read assay protocol. We checked the specificity of the UCP–Ag NC nanoprobe toward biothiols by measuring the responses of the probe to different species with the same experimental conditions and procedures. The probe showed positive responses to thiol-containing biomolecules, but no response to thiol-free species, including biomolecules, metal ions, and H_2O_2 (see Figure S11). Furthermore, the photostability and thermal stability of the nanoprobe were investigated. Under continuous irradiation with a 980 nm laser with a power density of 0.2 W cm^{-2} for 2 h, no evident change in the emission of the nanoprobe was observed (see Figure S12a). Also, incubation of the nanoprobe at 37 °C for 1.5 h did not lead to much change in the signal (see Figure S12b). These results indicate excellent stability of the probe and its suitability for long-term observation in bioimaging.

To investigate the biological application of the UCP–Ag NC nanoprobe, we then utilized it to monitor the fluctuation of intracellular biothiol levels in living cells. Upon endocytosis, the microenvironmental pH value of the probe may vary from 7.2 to approximately 4.5. Therefore, we first examined the response of the nanoprobe to the pH value. The emission intensity of the nanoprobe showed only a slight increase as the pH value decreased (see Figure S13). The biocompatibility of the nanoprobe was then assessed. The cytotoxicity was estimated by the standard 3-(4,5-dimethylthiazol-2-yl)-2,5-diphenyltetrazolium bromide (MTT) assay. We incubated cells with varying amounts of the nanoprobe for 24 h at 37 °C and found that a cell viability of greater than 90% was maintained in the presence of the probe at a concentration of 100 μg mL^{-1}, which is the amount we used in fluorescence microscopy experiments (see Figure S14). Thus the probe showed low toxicity toward cultured cell lines under the experimental conditions. Furthermore, the Z-scanning confocal imaging of cells clearly showed a stepwise increase in the distribution of probes within the cells. This result verifies the efficient uptake of the nanoprobe into the cytosol of living cells (see Figure S15). For the detection of biothiols, a group of HeLa cells were directly incubated with the nanoprobe (100 μg mL^{-1}) for 1.5 h. The cells exhibited

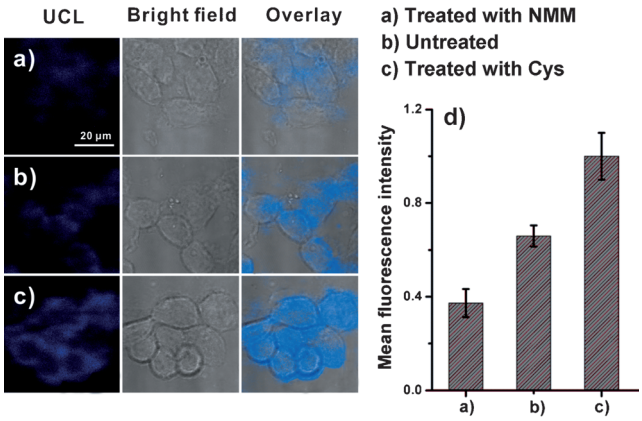

Figure 3. Confocal microscopic images of Hela cells incubated with the UCP–Ag NC nanoprobe (100 μg mL^{-1}). a, c) Hela cells were incubated with 1 mM NMM (a) or 0.5 mM Cys (c) for 1 h before incubation with the nanoprobe. b) Cells were incubated with the nanoprobe without pretreatment. d) Normalized average upconversion luminescence intensities in (a–c). All images have the same scale bar (20 μm).

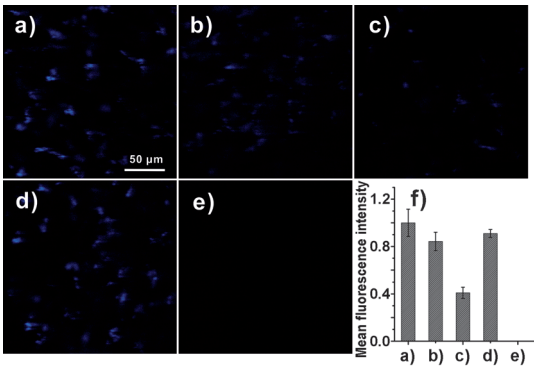

Figure 4. a–e) UCL images of liver tissue sections of mice injected with medicine and the nanoprobe. a–c) Mice injected with APAP (a: 0 mg kg^{-1}, b: 100 mg kg^{-1}, c: 300 mg kg^{-1}) for 30 min before the injection of the nanoprobe. d) Mice pretreated with α-lipoic acid (20 mg kg^{-1}) for 1 h before the injection of APAP (300 mg kg^{-1}) and the nanoprobe. e) Mice injected with physiological saline without the nanoprobe. f) Normalized average upconversion luminescence intensities in (a–e). All images have the same scale bar (50 μm).

moderate emission of UCPs in the 400–500 nm channel (Figure 3b), thus suggesting the recognition of intracellular biothiols. To see whether the probe could respond to changes in the intracellular biothiol level, two control groups of HeLa cells were separately pretreated with 0.5 mM exogenous Cys or 1 mM *N*-methylmaleimide (NMM), which acts as a biothiol-depleting agent, followed by incubation with the nanoprobe (100 μg mL^{-1}). The cells treated with NMM exhibited weakened UCP emission, whereas those pretreated with external Cys showed significantly increased luminescence (Figure 3a,c). These results confirmed the ability of the nanoprobe to discriminate different concentration levels of intracellular biothiols (the quantitative intensities of UCP emission are compared in Figure 3d).

To further evaluate whether the nanoprobe can be transported into organs in the living body and detect targets in vivo, we used the nanoprobe to monitor the liver biothiol content in a mouse model. The use of excessive amounts of acetaminophen (APAP), a safe painkiller, can cause severe liver damage[18] and the depletion of glutathione (GSH) in liver cells.[19] It was previously reported that this decrease in the GSH level can be suppressed by pretreatment with α-lipoic acid (α-LA).[20] Thus, we performed a UCL imaging study to monitor APAP-induced hepatotoxicity and the protective effect of α-LA in association with alterations in the GSH level of liver tissue. The liver tissue of the mice injected with the nanoprobe exhibited clear upconversion luminescence (Figure 4a), whereas the liver tissue of mice injected with only physiological saline (without the nanoprobe) showed no UCL signal (Figure 4e). These results reveal the near-zero autofluorescence from liver-tissue samples under irradiation with NIR light and the accumulation of the UCP–Ag NC nanoprobe in the livers of mice. Treatment of the mice by intravenous injection with APAP resulted in a significant decrease in the luminescence intensity, and the degree of the decrease in GSH was dependent on the dosage of APAP (Figure 4a–c). For a mouse pretreated with α-LA before the injection of APAP, the luminescence intensity did not change significantly (Figure 4a,d), thus verifying the protective effect of α-LA on the liver. The emission intensities of the samples are also quantitatively illustrated and compared in Figure 4f. Besides the above model for biothiol depletion in liver, we also used the UCP–Ag NC nanoprobe in another mouse model to detect promotion of the biothiol level. Previous studies have shown that the GSH levels in liver cancer and regenerated liver tissue are higher than in normal tissue.[21] We thus compared the UCL intensity of the nanoprobe in livers from normal and tumor-xenograft mice. Confocal fluorescence imaging of the tissues (see Figure S16) showed that, as anticipated, the upconversion luminescence in normal liver tissue was lower than that in xenograft liver tissue. All the above results indicate that the UCP–Ag NC nanoprobe can be an effective in vivo probe for the study of specific physiological processes.

In summary, we have demonstrated the capability of ultrasmall silver nanoclusters as the energy acceptor of upconversion-phosphor-based nanoprobes. To the best of our knowledge, noble-metal nanoclusters have not been used previously as the energy acceptors of UCPs. A LRET-based NIR nanoprobe was constructed in a straightforward way by decorating UCPs with Ag NCs. The molecule-like properties of the few-atom Ag NCs endowed the nanoprobe with both favorable LRET efficiency and good water solubility and biocompatibility. A rapid and reliable mix-and-read protocol can be used for target assays with the probe in solution. Moreover, the nanoprobe based on ultrasmall Ag NCs is suitable for use in living systems. As Ag NCs and other metal nanoclusters can be readily grown on various templates, our present strategy can be generalized to construct other nanoprobes combining UCPs and metal NCs by the use of other templates for NC growth.

Keywords: luminescence · metal clusters · nanostructures · probes · upconversion

How to cite: *Angew. Chem. Int. Ed.* **2015**, *54*, 5323 – 5327
Angew. Chem. **2015**, *127*, 5413 – 5417

[1] a) Q. Ju, D. Tu, Y. Liu, R. Li, H. Zhu, J. Chen, Z. Chen, M. Huang, X. Chen, *J. Am. Chem. Soc.* **2012**, *134*, 1323 – 1330; b) M. Haase, H. Schäfer, *Angew. Chem. Int. Ed.* **2011**, *50*, 5808 – 5829; *Angew. Chem.* **2011**, *123*, 5928 – 5950; c) D. E. Achatz, R. J. Meier, L. H. Fischer, O. S. Wolfbeis, *Angew. Chem. Int. Ed.* **2011**, *50*, 260 – 263; *Angew. Chem.* **2011**, *123*, 274 – 277; d) Q. J. Liu, Y. Liu, W. Bu, J. Bu, Y. Sun, J. Du, J. Shi, *J. Am. Chem. Soc.* **2014**, *136*, 9701 – 9709; e) L. Li, R. Zhang, L. Yin, K. Zheng, W. Qin, P. R. Selvin, Y. Lu, *Angew. Chem. Int. Ed.* **2012**, *51*, 6121 – 6125; *Angew. Chem.* **2012**, *124*, 6225 – 6229; f) R. J. Meier, J. M. Simbürger, T. Soukka, M. Schäferling, *Anal. Chem.* **2014**, *86*, 5535 – 5540.

[2] a) L. Yao, J. Zhou, J. Liu, W. Feng, F. Liu, *Adv. Funct. Mater.* **2012**, *22*, 2667 – 2672; b) Y. Cen, Y. M. Wu, X. J. Kong, S. Wu, R. Q. Yu, X. Chu, *Anal. Chem.* **2014**, *86*, 7119 – 7127; c) J. Liu, Y. Liu, Q. Liu, C. Li, L. Sun, F. Li, *J. Am. Chem. Soc.* **2011**, *133*, 15276 – 15279; d) Q. Liu, J. Peng, L. Sun, F. Li, *ACS Nano* **2011**, *5*, 8040 – 8048; e) L. Zhao, J. Peng, M. Chen, Y. Liu, L. Yao, W. Feng, F. Li, *ACS Appl. Mater. Interfaces* **2014**, *6*, 11190 – 11197.

[3] S. Han, R. Deng, X. Xie, X. Liu, *Angew. Chem. Int. Ed.* **2014**, *53*, 11702 – 11715; *Angew. Chem.* **2014**, *126*, 11892 – 11906.

[4] a) P. Zhang, S. Rogelj, K. Nguyen, D. Wheeler, *J. Am. Chem. Soc.* **2006**, *128*, 12410 – 12411; b) Z. Chen, H. Chen, H. Hu, M. Yu, F. Li, Q. Zhang, Z. Zhou, T. Yi, C. Huang, *J. Am. Chem. Soc.* **2008**, *130*, 3023 – 3029; c) T. Rantanen, M. L. Järvenpää, J. Vuojola, K. Kuningas, T. Soukka, *Angew. Chem. Int. Ed.* **2008**, *47*, 3811 – 3813; *Angew. Chem.* **2008**, *120*, 3871 – 3873.

[5] a) S. Wu, N. Duan, X. Ma, Y. Xia, H. Wang, Z. Wang, Q. Zhang, *Anal. Chem.* **2012**, *84*, 6263 – 6270; b) Y. Wang, P. Shen, C. Li, Y. Wang, Z. Liu, *Anal. Chem.* **2012**, *84*, 1466 – 1473.

[6] a) L. Wang, R. Yan, Z. Huo, L. Wang, J. Zeng, J. Bao, X. Wang, Q. Peng, Y. Li, *Angew. Chem. Int. Ed.* **2005**, *44*, 6054 – 6057; *Angew. Chem.* **2005**, *117*, 6208 – 6211; b) M. Wang, W. Hou, C. Mi, W. Wang, Z. Xu, H. Teng, C. Mao, S. Xu, *Anal. Chem.* **2009**, *81*, 8783 – 8789.

[7] R. Deng, X. Xie, M. Vendrell, Y. T. Chang, X. Liu, *J. Am. Chem. Soc.* **2011**, *133*, 20168 – 20171.

[8] a) I. Díez, R. Ras, *Nanoscale* **2011**, *3*, 1963 – 1970; b) A. Latorre, A. Somoza, *ChemBioChem* **2012**, *13*, 951 – 958; c) S. Choi, R. Dickson, J. Yu, *Chem. Soc. Rev.* **2012**, *41*, 1867 – 1891; d) X. Liu, F. Wang, R. Aizen, O. Yehezkeli, I. Willner, *J. Am. Chem. Soc.* **2013**, *135*, 11832 – 11839.

[9] a) T. Chen, Y. Hu, Y. Cen, X. Chu, Y. Lu, *J. Am. Chem. Soc.* **2013**, *135*, 11595 – 11602; b) L. Zhang, J. Zhu, S. Guo, T. Li, J. Li, E. Wang, *J. Am. Chem. Soc.* **2013**, *135*, 2303 – 2406; c) H.-C. Yeh, J. Sharma, I.-M. Shih, D. M. Vu, J. S. Martinez, J. H. Werner, *J. Am. Chem. Soc.* **2012**, *134*, 11550 – 11558; d) L. Shang, S. Dong, G. U. Nienhaus, *Nano Today* **2011**, *6*, 401 – 418.

[10] Y. Xiao, F. Shu, K.-Y. Wong, Z. Liu, *Anal. Chem.* **2013**, *85*, 8493 – 8497.

[11] a) N. Oien, L. Nguyen, F. Jernigan, M. Priestman, D. Lawrence, *Angew. Chem. Int. Ed.* **2014**, *53*, 3975 – 3978; *Angew. Chem.* **2014**, *126*, 4056 – 4059; b) S. Jiang, Y. Zhang, *Langmuir* **2010**, *26*, 6689 – 6694.

[12] F. Auzel, *Chem. Rev.* **2004**, *104*, 139 – 173.

[13] a) X. Yuan, Y. Tay, X. Dou, Z. Luo, D. T. Leong, J. Xie, *Anal. Chem.* **2013**, *85*, 1913 – 1919; b) B. Han, E. Wang, *Biosens. Bioelectron.* **2011**, *26*, 2585 – 2589.

[14] a) J. Lee, C. Lim, Y. Tian, J. Han, B. Cho, *J. Am. Chem. Soc.* **2010**, *132*, 1216 – 1217; b) X. Chen, Y. Zhou, X. Peng, J. Yoon, *Chem. Soc. Rev.* **2010**, *39*, 2120 – 2135.

[15] Q. Yuan, Y. Wu, J. Wang, D. Lu, Z. Zhao, T. Liu, X. Zhang, W. Tan, *Angew. Chem. Int. Ed.* **2013**, *52*, 13965 – 13969; *Angew. Chem.* **2013**, *125*, 14215 – 14219.

[16] M. S. Bootharaju, T. Pradeep, *Langmuir* **2013**, *29*, 8125 – 8132.

[17] R. Arppe, T. Näreoja, S. Nylund, L. Mattsson, S. Koho, J. M. Rosenholm, T. Soukka, M. Schäferling, *Nanoscale* **2014**, *6*, 6837 – 6843.

[18] C. Saito, C. Zwingmann, H. Jaeschke, *Hepatology* **2010**, *51*, 246 – 254.

[19] a) D. B. Mitchell, D. Acosta, J. V. Bruckner, *Toxicology* **1985**, *37*, 127 – 146; b) J. Yin, Y. Kwon, D. Kim, D. Lee, G. Kim, Y. Hu, J. H. Ryu, J. Yoon, *J. Am. Chem. Soc.* **2014**, *136*, 5351 – 5358.

[20] A. O. Abdel-Zaher, R. H. Abdel-Hady, M. M. Mahmoud, M. M. Y. Farrag, *Toxicology* **2008**, *243*, 261 – 270.

[21] Z. Z. Huang, C. Chen, Z. Zeng, H. Yang, J. Oh, L. Chen, S. C. Lu, *FASEB J.* **2001**, *15*, 19 – 21.

Received: January 1, 2015
Revised: February 10, 2015
Published online: March 5, 2015

